Bachelor Degree Project

UNIVERSITY OF SKÖVDE

FUSION PROTEIN

Construction of a fusion protein for anchoring the inflammatory receptor NLRP3 to the cell membrane

Bachelor Degree Project in BV506G
G2E 30 credits
Spring term 2019

Version 1.0

Author: Ling, Rebecca
Email: a16rebli@student.his.se
Bioscience - Molecular Biodesign

Supervisor: Edjebäck, Mikael
Email: mikael.edjeback@his.se
Supervisor: Herring, Matthew
Email: matthew.herring@his.se
Examiner: Fagerlind, Magnus
magnus.fagerlind@his.se

School of Bioscience
University of Skövde
Högskolevägen 3
Box 308
541 45 Skövde

Abstract

The innate immune system are a cooperation of many components – receptors being one of them. Both membrane-bound and cytosolic receptors play a large role in the defence system against pathogens and danger. NLRP3 is a receptor which assembles a protein complex called inflammasome in response to cytosolic stress and is responsible for many autoimmune diseases if it malfunctions. The activation of the NLRP3 inflammasome leads to secretion of inflammatory cytokines and in many cases to programmed cell death. The structure, function and activation of the NLRP3 inflammasome is still not fully understood and the urge to understand the mechanisms behind are important for future medical improvements. The aim was to anchor the NLRP3 inflammasome by the cell membrane - By Overlap PCR, the NLRP3 cDNA was fused extracellular and trans-membrane parts of the TLR4 cDNA to anchor the NLRP3 to the membrane and in turn analyse the inflammasome with LPI™ technology. Multiple primers and a TLR4 nucleotide were designed and the NLRP3 was amplified with specific overhangs by PCR. The fusion protein was successfully linked together by Overlap PCR but not confirmed by sequencing. The gene fusion demands high quality primers for amplification and further evaluation must be made to the details of the laboratory. To anchor the protein complex to the cell membrane, continue to be of full importance and can be an asset in many structural studies and biopharmaceuticals trials.

Keywords: NLRP3 inflammasome, Overlap PCR, Fusion Protein, LPI™ technology

Contents

Abbreviations

CAPS	Cryo pyrin-associated periodic syndromes
DAMPs	Damage associated molecular patterns
DC	Dendritic cells
LRRs	Leucine rich repeats
NEK7	NIMA-related kinase 7
NLR	Nucleotide-binding oligomerization-like receptors
NLRPs	NOD-like receptors with pyrin
OE-PCR	Overlap extension polymerase chain reaction
PAMPs	Pathogen associated molecular patterns
PRRs	Pattern recognition receptors
PYCARD	Adapter apoptosis-associated speck-like protein with a C-terminal caspase recruitment domain
ROS	Reactive oxygen species
T2D	Type 2 diabetes
TLR	Toll-like receptors
PCR	Polymerase chain reaction

1. Introduction

1.1 Background

1.1.1 Inflammation and the immune system

The immune system response to pathogens is a cooperation between the innate and adaptive immune systems. The adaptive immune system has receptors that can both distinguish self from non-self and save the encountering to a memory ensuring a more efficient response next time the intruder interact with the cells. This side of the immune system delivers advantages in response rate and proliferation capacity (Yatim & Lakkis, 2015). The innate immune system in the other hand is an already implemented defence system present in most cells, with or without infection. By encountering certain danger signals or pathogens the innate system is the first to be activated. The rapid response fights infection and different tissue damages and the efficiency of the response is highly important as bacteria has a fast doubling time. The innate immune response has many components and a cellular system which mainly consist of phagocytic cells, antigen presenting cell and killing cells (Hato & Dagher, 2015). Two components called monocytes and neutrophils react quickly to local infection and are effective killers by releasing substances to damage and then engulf (phagocytosis) pathogens (Nicholson, 2016). These defence mechanisms are encoded in the germline. Many components that are established to fight infection are also responsible to maintain normal tissue homeostasis and eliminating apoptotic cells. The innate immune system is not enough for complete protection and has a no memory against pathogens which can cause receptors to lack the knowledge to distinguish more than self from non-self and therefore crucial to cooperate with the adaptive immune system (Yatim & Lakkis, 2015). The monocytes and dendritic cells (DC) of the innate immune system circulate in the blood or inside the tissues and are bone marrow derived (Wacleche, Tremblay, Routy & Ancuta, 2018). Furthermore, the monocytes and macrophages co-exist and have crucial roles in the immune system. Monocytes/macrophages got the ability to digest and present antigens to immune cells of the adaptive immune system – and therefore allowing interaction between the two immune systems (Prame, Nicholls, & Wong, 2018).

1.1.2 Recognition systems - Receptors

The innate immune system can by different recognition systems recognize common structural features of a wide range of microorganisms. These recognition systems allow the system to locate and identify intruders and determine both the pathogenicity and viability. The cells that encounter infection produce a set of cytokines which stimulate cell division which in turn produce a cascade of cytokines to activate effector responses. These specialized recognition systems detect pathogen associated molecular patterns (PAMPs) from common components of bacteria, viruses or funghi (e.g. lipopeptides, lipopolysaccharides or dsRNA) (Iwasaki & Medzhitov, 2015). Toll-like receptors (TLRs) recognizes ligands and induce inflammatory-cascades. Beside the membrane-bound receptors there are receptors which are located inside the cell and all these receptors together are called pattern recognition receptors (PRRs) (Hato & Dagher, 2015). TLRs are membrane-bound glycoproteins often expressed in dendritic cells and macrophages and can induce different cascades depending on the receptor. TLR4 is part of the family and can activate multiple cascades and are therefore unique (Hato & Dagher, 2015). The TLR4 mediate response to bacterial LPSs lipopolysaccharides (LPS) in cooperation between the MD-2 and CD14 proteins (Tatematsu et al., 2016), it can also effect the TLR4 to be involved in an LPS-independent response, stimulate NF-kappa-B expression and formation of a TLR4 and TLR6 complex – which all trigger inflammatory response (Medzhitov, Preston-Hurlburt, & Janeway, 1997; Schmidt et al., 2010; Estruch et al., 2013).

Another major class are called Nucleotide-binding domain and leucine-rich repeat (NOD-like Receptors, NLRs) and acts as cytosolic sensors. Many of the NLRs are associated with multiple functions in both immune responses and dysfunctions associated with multiple diseases. The NLRs detect damage associated molecular patterns (DAMPs) and PAMPs. DAMPs could be crystals, pore-forming bacterial toxins and protein aggregates which indicate damage to the cell surface and PAMPs are molecules that warn for potential danger (Ellwanger et al., 2018).

1.1.3 Inflammasomes and the NLRP3

One family of the NLRs are called NLRPs e.g. NLRs with a pyrin domain. Some of these NLRPs can induce formation of a protein signalling complex called inflammasome (Moossavi, Parsamanesh, Bahrami, Atkin, & Sahebkar, 2018; Iwasaki & Medzhitov, 2015; Groslambert & Py, 2018). The inflammasomes are assembled inside the cytosolic compartment and are activated in response to danger (Próchnicki, Mangan, & Latz, 2016). These multi-protein complexes can trigger inflammatory pathways through various activation processes. NLRP1, NLRP3, NLRC4 and non-NLR receptors, such as AIM2 and IFI16, are examples on proteins which form these complexes (Davis, Wen, & Ting, 2011). One of these intracellular protein complexes, the NLRP3, is the inflammasome most widely characterized. The NLRP3 protein is predominantly expressed in macrophages and is often located in the cytosol or on the endoplasmic reticulum. NLRP3 is also expressed in dendritic cells, killer cells, chondrocytes and monocytes at different levels (Nakanishi et al., 2017; Manji et al., 2002; Feldmann et al., 2002). The NLRP3 inflammasome consist of an adaptor (ASC or PYCARD - adapter apoptosis-associated speck-like protein with a C-terminal caspase recruitment domain), a sensor protein (NLR) and an effector (caspase-1), see Figure 2F. Because of the highly diverse onset of regulation it has been proposed that the activation of the NLRP3 may include a two-step process. Primary signalling depends on an initial stimulus (e.g. PAMPs) which then in combination with a second stimuli (e.g. DAMPs) could lead to formation of the active NLRP3 complex. (Baldwin et al., 2018).

1.1.3 Inflammasome activation

The first signal is often an inflammatory stimulus which causes a priming event. The priming involves induced and mediated pathways of pro-IL-1B expression and NF-KB-mediated NLRP3 expression (Yang, Wang, Kouadir, Song, & Shi, 2019). With a second stimuli it activates the NLRP3 inflammasome assembly by catalysing the NLRP3 to oligomerize and to recruit the ASC (Figure 1) (Liu & Cao., 2016). The pyrin domain of NLRP3 bind to the pyrin domain of the ASC and after the recruitment, the ASC binds the cysteine protease pro-caspase-1 via their caspase recruitment domain to form the complex. This causes autocatalytic cleavage of the pro-caspase-1 to the active form caspase-1. In turn, this causes proteolytic activation of pro-inflammatory cytokines such as mature IL-1B and IL-18, and their secretion, which in many cases lead to pyroptosis (Jo et al., 2016). The pyroptosis is upon activation of the inflammasome promoted by the N-terminal domain of gasdermin D, which can form pores in the cell membrane (Yang, Wang, Kouadir, Song, & Shi, 2019). The molecular mechanisms which is controlling the NLRP3 inflammasome activation is still not completely understood but are accepted that exogenous activators are not interacting directly with the NLRP3 (Groslambert & Py, 2018). Without any immune activator, the NACHT domain and leucine-rich repeats (LRRs) to have an internal interaction and by that prevent inflammasome assembly (Inoue & Shinoharashao, 2013). By the secondary step or stimuli, the NLRP3 allow activation by breaking the internal interaction between the NACHT and LRRs. As mentioned before the PAMPs and DAMPs can trigger an activation response, as well as extracellular ATP which acts as an agonist (promotes activity) which can induce efflux of potassium causing activation (Shao, Xu, Han, Su, & Liu, 2015). The onset of the NLRP3 are dependent on many reactions and ion fluxes may be important, but not mandatory or dependent for activation (Yang, Wang, Kouadir, Song, & Shi, 2019).

The NLRP3 inflammasome can as said be triggered by multiple DAMPs e.g. environmental irritants, mitochondrial damage and lysosomal disruption (Shao, Xu, Han, Su, & Liu, 2015; Miao et al., 2014). The lysosomal disruption can be caused by the conversion of soluble ligands to crystals or fibrils which in turn can contribute to the NLRP3 activation and induce production of interleukin-1β, known for linkage to many inflammatory diseases (Sheedy et al., 2013). Altered glycolysis and oxidative phosphorylation may also influence certain mechanisms which are important in NLRP3 priming. Example could be new fatty synthesis, citrate and succinate utilization and reactive oxygen species (ROS) (Elliot & Sutterwala, 2016). The activations signals are concluded to be different kinds of cytosolic stress and the formation requires the two-step process of the multiple activators (Groslambert & Py., 2018).

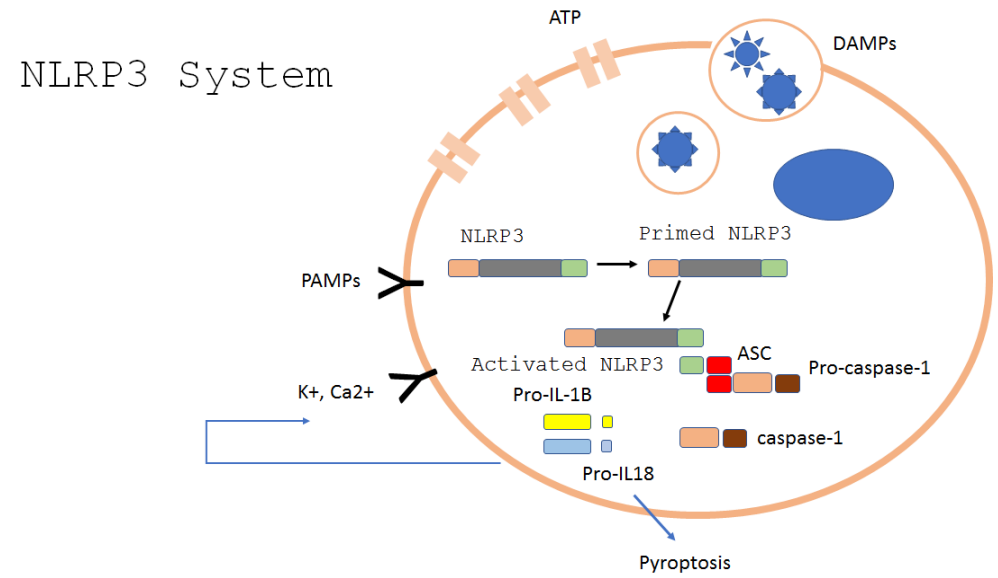

Figure 1. Simple schematic overview of the NLRP3 components and assembly. Different mechanisms which affect the activation included the effect of the pathway. Modified of multiple pictures. Credit to Gorslambert & Py, 2018; Yang, Wang, Kouadir, Song, & Shi, 2019; Jo et al, 2016; Cassel & Sutterwala, 2010

1.1.4 NLRP3 assembly

The structure of NLRP3 is not fully known and there are multiple theories on how it may be composed. Evidence from the structures of other NLRs gave the hypothesis that the inflammasomes are built like a bicycle wheel with 7 different spokes, called “spoked wheel” (Figure 2A & 2E) (Faustion et al., 2007). The inner centre consist of caspase-1 with connection to the NLRP3 spokes through the ASC. Another model is called “branching tree model” and have a build-on heptametrical structure with recruited caspase-1 as branches (Figure 2B). Here the ASC is a fibrous trunk with an NLRP3 root. The third model is called a “layered speck” where caspase-1 and IL-1B are retained in the core of the structure (Figure 2C) (Cai et al., 2014). The NLRP3 is stated to surround the core with a protective layer of ASC on the outer membrane (Elliot & Sutterwala, 2016). Another model is called the “Sandwich”, which indicates that the NLRP3 is forming a sandwich-like structure bound to the ER (Figure 2D (Franklin et al., 2014). However, the spoke-like wheel organization is better supported by scientific evidence than the other proposed theories (Elliot & Sutterwala, 2016).

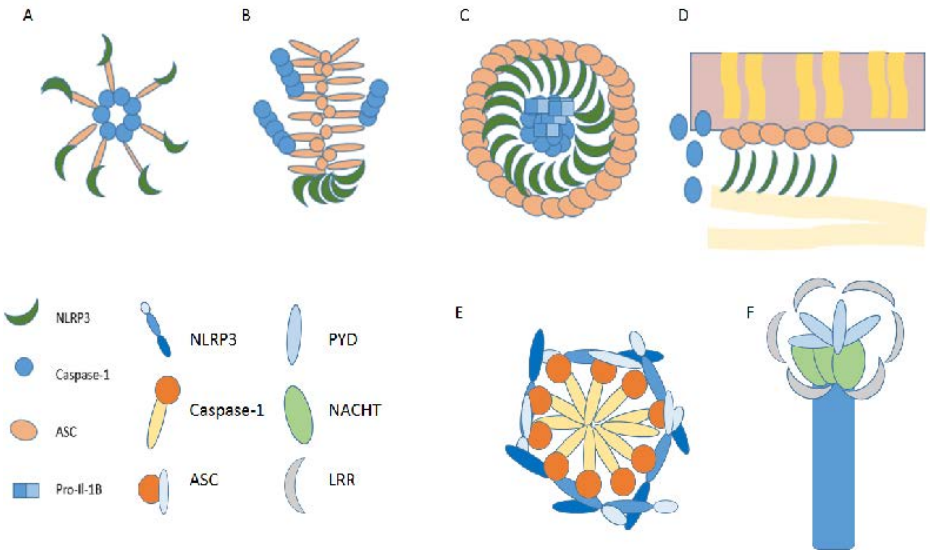

Figure 2. Models of the NLRP3 and NLRP3 inflammasome complex structure. (A) Spoked wheel, (B) branching tree, (C) layered speck, (D) sandwich, (E) Version of spoked wheel, (F) NLRP3 prior assembly. Modified of multiple pictures. Credit to; Elliot & Sutterwala, 2016; Shao, Xu, Han, Su, & Liu, 2015; Schmith et al, 2016.

1.1.5 Diseases and inhibitors

Activation of the NLRP3 inflammasome can be protective during an infection but can in unregulated cases cause unintended pathology and disease (Elliot & Sutterwala, 2016). To comprehend the functions and understand the advanced mechanisms of NLRP3 activation is highly significant because of the broad involvement in several human diseases and pathological conditions (Próchnicki, Mangan, & Latz, 2016). The NLRP3 inflammasome activation is associated and proved to be responsible or partly involved in chronic inflammatory, auto-inflammatory, autoimmune and metabolic diseases which indicates that the regulation of the inflammasome is of central (Kyeong et al., 2016; Uniprot, Q96P20). The NLRP3 complex also has a genetic association with hereditary auto-inflammatory diseases. The different diseases, also known as cryo pyrin-associated periodic syndromes (CAPS), are Muckle-Wells syndrome, neonatal-onset multisystem inflammatory disease and familial cold auto-inflammation syndrome. Furthermore, the NLRP3-mediated inflammation has also been linked to numerous diseases including Alzheimer´s, Parkinson´s, type 2 diabetes and other multifactorial diseases (Groslambert & Benedicte, 2018). There are inhibitors that target the IL-1B secretion but most of these are not efficient or specific. Therefore, inhibitors that target the NLRP3 could be the best choice when it comes to related diseases. MCC950 which is a small inhibitor molecule seems to prevent NLRP3-induced ASC oligomerization and in turn inhibit both NLRP3 activation and IL-1B secretion (Yang, Wang, Kouadir, Song, & Shi, 2019). Another inhibitor is called CY-09 which binds to the ATP site of the NLRP3 NACHT domain. The binding seemed to affect the NLRP3 inflammasome activation and had success in treating diseases as T2D (type 2 diabetes) and CAPS (cryo pyrin-associated periodic syndrome) (Jiang et al., 2017). By blockage of NLRP3 activation it would be possible to inhibit the release of IL-1B and IL-18 which in turn would prevent pyroptosis. Biological inhibitors available today is not sufficient for total blockage and serve lower value due to the high cost (Baldwin et al., 2018).

1.1.6 Overlap extension PCR

The original OE-PCR was used for splicing without the presence of restriction enzymes but can be applied on long-length DNA fusion and gene mutation. The PCR approach was initially employed to be able to fuse two or three independent fragments and it has successfully assembled up to four fragments (Ho, Hunt, Horton, Pullen, & Pease, 1989; Shevchuk et al., 2004). The general hypothetical principle of the method is divided into two steps. The primary step involves amplifying the independent fragments with necessary overlap sequences which in the secondary step will be matching sequences and extend and create full synthetized hybrid DNAs (Luo, Liu, Lin, Kabir, & Su, 2013). The PCR products of each step can be used as a template directly without purification in-between steps (Ahn, Keum, & Kim, 2011). The extension of the overlapping segments requires internal primers which generate the overlapping and complementary 3' ends. Furthermore, two flanking primers are necessary which can add enzyme restriction sites or other sequences for future purpose which in turn generate a full-length DNA product (Heckman & Pease, 2007).

1.3 Research problem and aim

Even though the main functions of NLRP3 are widely characterized there is still many molecular mechanisms behind the NLRP3 assembly and activation that remain unknown. Further studies on the composition and function of the NLRP3 inflammasome could provide knowledge behind the mechanisms responsible for over activity and how mutations cause changes in the composition and in turn explain different disease and pathological states. Different approaches can be used to capture the inflammasome complex in order to characterize it. One technique is Lipid-based Protein Immobilization Technology (LPI™) developed by Nanoxis. This technique has been developed for membrane-bound proteins. In order to make the NLRP3 inflammasome membrane bound, the aim was to construct a fusion protein between the NLRP3 protein and parts (signal peptide and membrane-bound part) of the TLR4 protein with the aim to bind the NLRP3 to the cell membrane. This is the first attempt of many and there is no prior work on the same fusion approach with NLRP3. This will enable more intense studies of the inflammasome structural composition which needs to be integrated with the molecular mechanisms. Hopefully this work can lead to better understanding of the NLRP3 inflammasome and ultimately contribute to treatment therapies in the future by analysis of negative regulators and signals of the inflammasome. It could potentially allow manipulation of the inflammasome to prevent multiple disease states (Jo, Kim, Shin, & Sasakawa, 2016).

2. Materials & Methods

One approach to fuse proteins together is by overlap extension PCR (OE-PCR) which was the chosen method to create the fusion construct. The reactions consist of generating DNA fragments with desired overlapping ends (see Figure 3) which will join the two fragments together (Hussain & Chong, 2016). The whole NLRP3 coding region was used as template and parts of the TLR4 coding region. The oligonucleotide was designed to include the signal peptide (for localization) and the transmembrane part of the TLR4. The fusion of the two genes would enable the anchoring of the NLRP3 to the cell membrane. As plasmids containing the both desired fragments were available, it was a more cost-efficient way to receive the two genes and order separate primers.

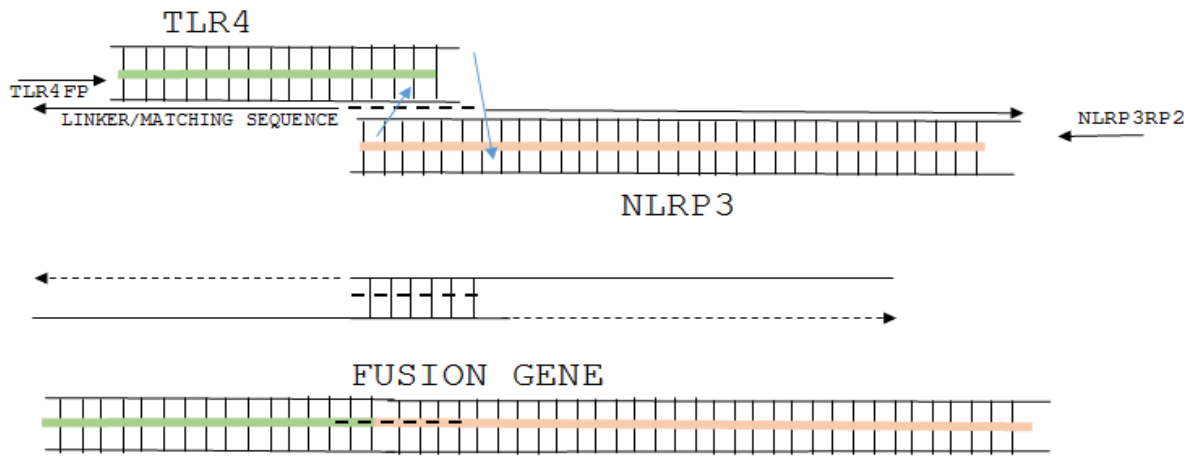

Figure 3. Schematic overview of OE-PCR performed with and without primers. The theory without primers is that the fragments with complementary ends prime each other. Top: with primers, Bottom: without primers

To be able to answer and reach the goals of the research problem the following experimental outline of the project was followed: (i) Design and synthesis of a fusion protein built of the NLRP3 and TLR4 protein (Appendix 8.2) with appropriate linker by OE-PCR, (ii) Transformation and sequencing of the fusion protein construct. All concept of the laboratory is presented (Figure 4) and described in detailed subsections below.

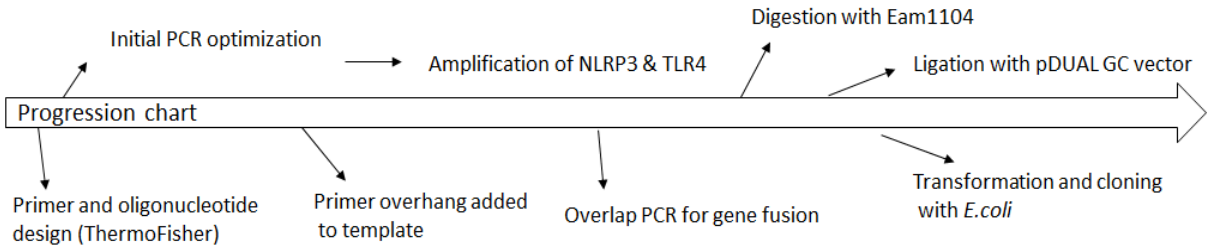

Figure 4. Progression chart of the main steps performed. Steps that has been omitted due to constraints are not included.

2.2 Oligonucleotide design

Oligonucleotide design was performed with the Primer-Blast tool (NCBI), Primer3 (Biotools) and Oligo Calc (Biotools). Parameters regarding the primer design were set with default values (size, GC content, etc.) All primers were investigated with different tools to ensure compatibility. Oligocalc (Biotools) was used to avoid self-complementarity, Reverse-Complement

(Bioinformatics) for right translation of sequences and BLAST for alignment between the sequences and the genes (NCBI).

To amplify the cloned full-length genes from the plasmid, available M13 universal primers (Invitrogen™) were first used. As these did not work new gene-specific primers (NLRP3FP0/RP0, TLR4FP/RP) were ordered for plasmids containing the TLR4 and NLRP3 genes (Table 1). The primers were designed for amplification of the full-length coding regions.

Table 1. Primers used in the PCR reactions. All primers shown from 5' to 3'.

Primer		Length (nt)	Melting Temp °	GC %
NLRP3 FP0	ATGAAGATGGCAAGCACCC	19	58.11	52.63
NLRP3 RP0	CTACCAAGAAGGCTCAAAGACG	22	59.00	50.00
TLR4 FP	ATGATGTCTGCCTCGCGCCTG	21	65.41	61.90
TLR4 RP	TCAGATAGATGTTCCTGCCAATTG	28	63.74	42.86
NLRP3 FP1	GGTTCTGGTGGAGGAGGTTCTATGAAGATGGCA	33	70.10	51.52
NLRP3 RP1	GGCGTCAT**CTCTTC**TAAGCTACTCAAAGACGACG	34	69.22	50.00
NLRP3 FP2	GGTTCTGGTGGAGGAGGTTCTATGAAGATGGCAAGC	36	71.85	52.78
TLR4syntFP	ACCTCTTCAATGATGTCTGCCTCGCGCCTGG	31	74	58.06
TLR4syntRP	AGAACCTCCTCCACCAGAACCGCCGCCTCC	30	76.9	66.67

* Underlined: overhangs, bold: Eam1104 specific cleavage site.

A second set of primers were designed with specific overhangs to be added to the NLRP3 sequence for the protein fusion (Table 1. The overlapping sequence was matching the sequence of the TLR4 design and was partly added (20nt) with one forward primer. The reverse primer was designed to include the Eam1104 cleavage site (CTCTTC) and a random sequence was added on the 3´end to adjust the GC content (NLRP3 RP1, Table 1). A second NLRP forward primer (NLRP3 FP2) was also designed and tested to increase binding efficiency (Table 2).

The cleavage sites for Eam1104 were added to the 5´end to the TLR4 and to the 3´end on the NLRP3 according to recommendations from the pDUAL GC Expression vector protocol (Agilent Technologies, Table 2).

Table 2. Eam1104 cleavage site and recommendations for plasmid insert.

Eam1104 cleavage site	Recommended insert
CTCTTCN▼	NN**CTCTTC**NATG cDNA insert CTTN**GAAGAG**NN
GAGAAGNNNN▲	NN**GAGAAG**NTAC cDNA insert GAAN**CTTCTC**NN

The desired TLR4 sequence with modifications designed and ordered (GeneArt™ Strings™ Invitrogen, Thermo Fisher Scientific). The sequence ordered contained TLR4 residues GC-AT with added Eam1104 cleavage-site, Enterokinase cleavage-site, TLR4 signal peptide and transmembrane sequence (Appendix 7.2), TEV-cleavage site and an overlapping sequence (common flexible linker: Gly-Gly-Gly-Gly-Ser n x 2) with NLRP3 (Figure 4). The cleavage sites of Enterokinase and TEV-cleavage sites was added to enable down-stream peptide-cleavage if desired. Eam1104 cleavage site was included for plasmid insertion and cloning and the overlapping sequence for successful protein fusion with the NLRP3 (Appendix 8.1). The STOP codon is at the end of the NLRP3 sequence for proper termination of translation.

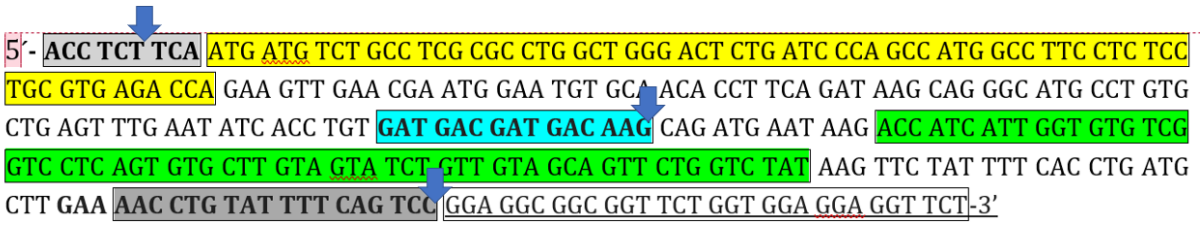

Figure 5. Designed TLR4 sequence. Grey: Eam1104 Cleavage site, yellow: signal peptide, blue: Enterokinase cleavage site, green: transmembrane sequence, dark grey: TEV-cleavage site, transparent: overlapping NLRP3 sequence. Arrows represent all cutting sites.

2.1 PCR reaction optimization

2.1.1 Detect the NLRP3 and TLR4 of unknown plasmids

PCR reactions were first performed to detect the presence of full-length NLRP3 and TLR4 cDNA in the available plasmids and to find the optimal parameters. The volumes used of plasmids containing the NLRP3 coding gene and the TLR4 coding gene was 10ng (TLR4) and 9.76 ng (NLRP3) concentration. The PCR reaction was set up according to the manufacturer protocol (Phusion High-Fidelity DNA Polymerase, NEB) in 50 µl reactions. Three replicates of each gene was set up with M13 universal primers (final concentration 0.5µM per primer) and the PCR cycle as listed in Table 3. Cutsmart buffer 100% was used for all PCR reaction with already added DMSO.

Table 3. PCR parameters - temperatures and time intervals. Program run for 30 cycles.

Initial denaturation	98°C	30 s
Denaturation	98°C	7 s
Annealing	65°C	20 s
Extension	72°C	22 s
Final extension	72°C	7 min

The PCR products of both the NLRP3 and TLR4 reactions was analysed by restriction enzyme digestion. The NLRP3 was digested with EcoNI and AvaI. The TLR4 was digested with EcoNI and Cas8I. CutSmart buffer (NEB) was used for all digestions with calculated 100% enzyme activity. The digestion was set up in 40 µl reactions according to the recommendations for the NEB enzymes. All enzymes where heat inactivated for 20 minutes in 65°C. Orange G Loading Dye (Bio-rad) was added to the samples which where run on 1 % agarose gels with TAE buffer (Appendix 8.3) and containing GelRed/GelGreen with 1 kb ladder (Biolabs New England). - The gel was run on around 95-110 voltage for 1.5 hours. The PCR described previously was further optimized according to Table 2. The DNA template amount was lowered to 5 ng in each reaction (recommended in protocol; 1pg -10ng). The PCR cycling protocol was also changed; lower annealing temperature, longer extension time, and shorter final extension.

Table 4. PCR parameters - temperatures and time intervals. Cycles made: 30.

Initial denaturation	98°C	30 s
Denaturation	98°C	10 s
Annealing	55°C	20 s
Extension	72°C	45 s
Final extension	72°C	5 min

Digestion was set up as 25µl reactions, with 500 ng PCR product in the reactions and incubation at 37° for 20 minutes. Results were analysed on an agarose gel as described above.

2.1.2 TOPO and pQETRI plasmids

The PCR was further optimized with a new PCR cycling protocol (Table 5) with primers from previous reactions (NLRP30, TLR4, Table 4) were used for new plasmids - pCR™-XL-2-TOPO vector (Invitrogen) containing the coding region of NLRP3 and pQE-TriSystem Vector (Qiagen) containing the coding region of TLR4. The primers were used in a final concentration of 0.5µM and the reaction was set up with 5 ng of plasmid DNA. Changes that was made; annealing gradient temperatures (61.1°, 65.2°, 68.9°, 71.1°C), extension 1 minute and final extension 10 minutes. The annealing temperature was set to a gradient to investigate annealing optimum based on the primers. Samples was prepared of each plasmid (NLRP3 & TLR4) and set up to the different annealing temperatures (Table 5). Nanodrop™ and Qubit 3.0 Fluorimeter (Qubit® dsDNA HS Assay Kit *0.2–100 ng, Life technologies) was used for all concentration and purity measurements. Results were analysed on an agarose gel as described previously.

Table 5. PCR parameters - temperatures and time intervals. Cycles made: 30.

Initial denaturation	98°C	30 s
Denaturation	98°C	10 s
Annealing	61.1°C, 65.2°C, 68.9°C, 71.1°C	20 s
Extension	72°C	1 min
Final extension	72°C	10 min

2.4 PCR amplification and overlap PCR

Further work was performed with the PCRBIO HiFI Polymerase according to the manufacturers protocol (PCRBIO-systems). Reagents set up: 1X PCRBIO Reaction Buffer, PCRBIO HiFi Polymerase, forward and reverse primers 0.4µM and 1.69 ng template DNA. The amplified NLRP3 from PCR optimization was used as template and PCR was performed to attach desired overhangs to the NLRP3. Multiple PCR strategies were tried to add the overhangs (Table 6). The primer concentration was 0.5µM for all attempts except the last one with two-step PCR which had 2 µM of each primer, same DNA amount was used in the reactions (1.69ng). All PCR products concentrations was measured, and results were analysed on an agarose gel as described previously but with Purple Loading Dye 6X (BioRads). One PCR reaction was also run with the TOPO-plasmid as template with annealing temperature of 65°C for 10 cycles than a gradient (65°C, 67°C, 69°C, 71.8°C, and 72.9°C) for 20 cycles, final extension 5 minutes and with 0.8 ng DNA in 20µl reactions.

Table 6. PCR settings for multiple PCR strategies. Changes made to the annealing temperatures and cycles.

Initial denaturation	98°C	30 s
Denaturation	98°C	10 s
Annealing	(70°C-71°C for 25 cycles) (touch-up; 5 cycles 55°C, 20 cycles 72°C) (touch-up; 5 cycles 60°C, 20 cycles gradient 62°C, 65.2°C, 68.9°C, and 71.1°C)(10 cycles 55°C, two-step 15 cycles 72°C)	20 s
Extension	72°C	1 min
Final extension	72°C	10 min

To fuse the TLR4 oligonucleotide with the NLRP3 product containing added overhangs from previous step. Adjusted parameters; annealing temperature gradient of 65°, 68.7° and 70.9°, a molar ratio of 1:10 of TLR4/NLRP3 was added (5ng/50ng), extension time 1.5 min, final extension time of 5 min. PCR reactions with and without[1] primers were set up for each annealing temperature. The concentration of the PCR products was measured and run on gel to confirm the expected fragment sizes and then purified. The process consists of binding DNA to a silica membrane followed by washing steps, and finally elution to receive purified isolated DNA (NucleoSpin Gel and PCR Clean-up, Macherey-Nagel).

The products from PCR reactions without primers were used for another PCR (10ng of each sample in 50ul and annelaing temperature of 68°. One new sample (50ul) was also set up with the same molar ratio but with a higher concentration (9ng TLR4 & 90 ng NLRP3) of template. The single sample was run without primers at 3 cycles of PCR with the settings; 72° annealing temperature and extension time for 5 minutes (Table 7). Primers were then added to the sample and the other samples joined the PCR. Changed settings: 68° annealing temperature for 15 s and run for 30 cycles. Further optimization lead to new samples set up accordingly to table 7 and the samples with new DNA were run for 2 cycles prior addition of primers. PCR parameters was changes: extension time 2 minutes and run for 30 cycles on an annealing gradient of 71° C and 73° C. All samples without primers were pooled together and purified to receive 30 µl of product which was used to proceed. Nanodrop™ and Qubit 3.0 Fluorimeter was used for all concentration and purity measurements

Table 7. Sample set up in multiple PCR events. Samples with new DNA was run for 2 cycles prior addition of primers and then all samples were run for 30 cycles

	Sample	**No primers**	**Primers new DNA**	**Primers fusion DNA**
DNA	TLR4	9 ng	1 ng	10 ng fusion DNA
	NLRP3	90 ng	9 ng	

2.5 Digestion with Eam1104 and ligation with pDUAL-GC vector

The fusion protein product and the pDUAL-GC expression vector (Genomics Agilent) was digested with Eam1104 (Eam1104 I protocol, Thermo Fisher) according to the manufacturer's instructions. Ligation was performed with T4 Ligase (New England Biolabs) followed the pDUAL-GC expression vector protocol. The plasmid was transformed into *E.coli*-DH5α- cells (Invitrogen) and plated overnight with LB-agar plates containing kanamycin 100ng/µl in 37°C, the manufacturer's instructions was used (Subcloning Efficiency™ DH5a Competent cells, Invitrogen).

2.9 Ethics

An ethical analyse is a strategy to determine the conflicts between the conducted project and the world or societies interests. The analysis is necessary to see if there are any different opinions of question in mind and to involve all effected aspects (SMER, 2018). As the production and transduction with a fusion protein result in genetically modified organisms there are different directives that has to be followed when the organisms are set to be let out in nature (Euro parliament's directives, 2001). This was not be the case as the use of bacteria was used in the lab and not produced for any purpose to affect the environment outside. This is enclosed use of genetically modified species and follow specific directives derived from the Environmental and energy department (2000). The stated laws demand an assessment of risks to determine a

[1] The DNA fragments in the reactions without the primers were supposed to prime each other and be extended.

classification of the project which involves; F-, L- and R-classification. The classification will determine the risk of affects to the environment or human health. It will also determine what safety measures has to be followed (Environmental and energy department, 2000). Accordingly, to the Swedish Work Environment Authority there are general recommendations when working with genetically modified Micro-organisms. As mentioned before a classification is needed and the University of Skövde has an L-classification which holds both number 1 and 2 in containment level. Security measures was considered as recommended from the level of classification. This involved labelling, waste handling, a contingency plan and avoid decontamination in closed measures (Swedish Work Environment Authority, 2011). No license must be applied for as the University of Skövde was the base of this project and classifications and licences are available.

3. Results

The products of the first PCR which was amplified to isolate the NLRP3, was loaded on gel. The expected fragments sizes for the NLRP3 and when digested are stated in Table 8.

Table 8. Gel electrophoresis 1%. Loaded samples with expected fragment sizes.

Well	**1**	**2**	**3**	**4**	**5**	**6**	**7**
Sample & enzyme	1 kb Ladder	NLRP3 cDNA(amplified)	EcoNI NLRP3	AvaI NLRP3	TLR4 cDNA(amplified)	EcoNI TLR4	Cas8I TLR4
Expected fragments	-	3111bp	1450bp, 1658bp	123bp 901bp 334bp 1750bp	2517bp	203bp 2314bp	1437bp 415bp 134bp 531bp

Many attempts lead to failure of both amplification of the NLRP3 and the TLR4 (Figure 6A). Further optimization showed distinct bands for all NLRP3 samples (Figure 6B) at 3 kb according to 1 kb ladder which was the expected fragment size. The optimum annealing temperature was found to be 71.1° C. The amplification of TLR4 gave no result and despite repeated PCR reactions there was still no success with the TLR4 amplification which in turn resulted in a decision to order a designed oligonucleotide for modified TLR4 sequence. Digestion was performed to confirm the amplified NLRP3 (Figure 6C). The fragment sizes agreed with sizes in Table 8. Next PCR reaction was performed to add the desired overhang sequences to the NLRP3. The experiment was not successful even though many different parameters and settings were performed (Figure 7D, Figure 7A, 7C).

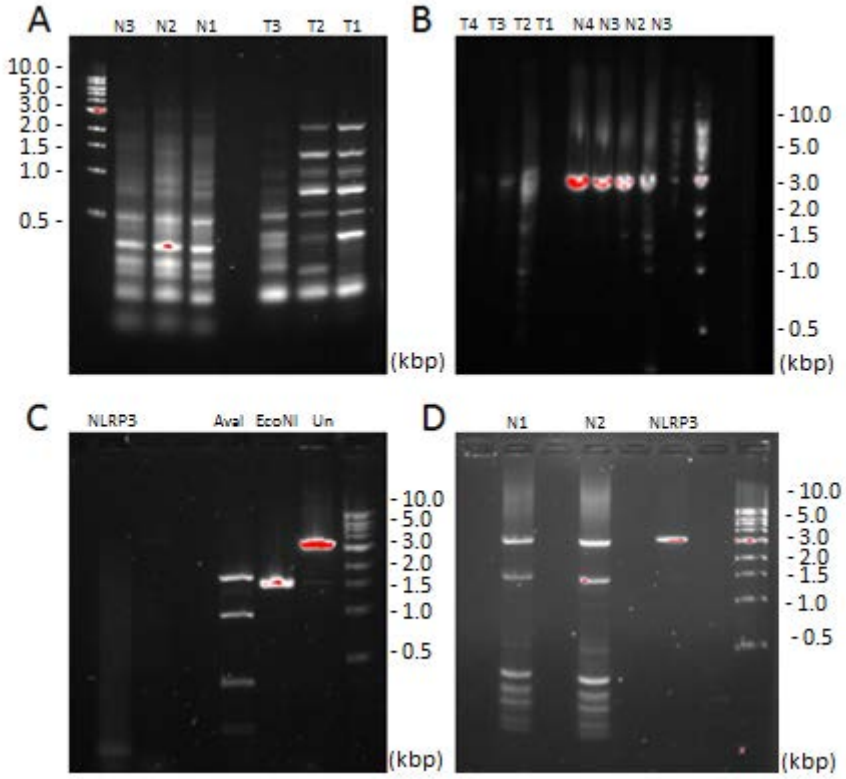

* N: NLRP3 PCR samples, T: TLR4 PCR samples, UN: Undigested NLRP3

Figure 6. Result of agarose gel electrophoresis of PCR amplifications. 1kb Ladder (Biolabs), A) Amplification and digestion of NLRP3 with AvaI, EcoNI and Cas8I, B) NLRP3 amplification, C) Digestion of NLRP3 with AvaI and EcoNI, D) The attempt to add overhangs to the NLRP3 was unsuccessful.

The amplification of the NLRP3 was repeated straight from the plasmid and gave a clear distinct band visible for sample 4 (Figure 7B) at an annealing temperature of 71.8° C. Only this sample gave desired result and was therefore repeated with exact same settings to confirm the laboratory success (Figure 7D). The NLRP3 was amplified with the overhang primers (NLRP3O_FP, NLRP3O_RP). The amount was enough for the overlap PCR which was set up to a Molar ratio of 1:10 (TLR4:NLRP3). All concentrations and purity levels were measured, and the essential ones are shown in Table 9.

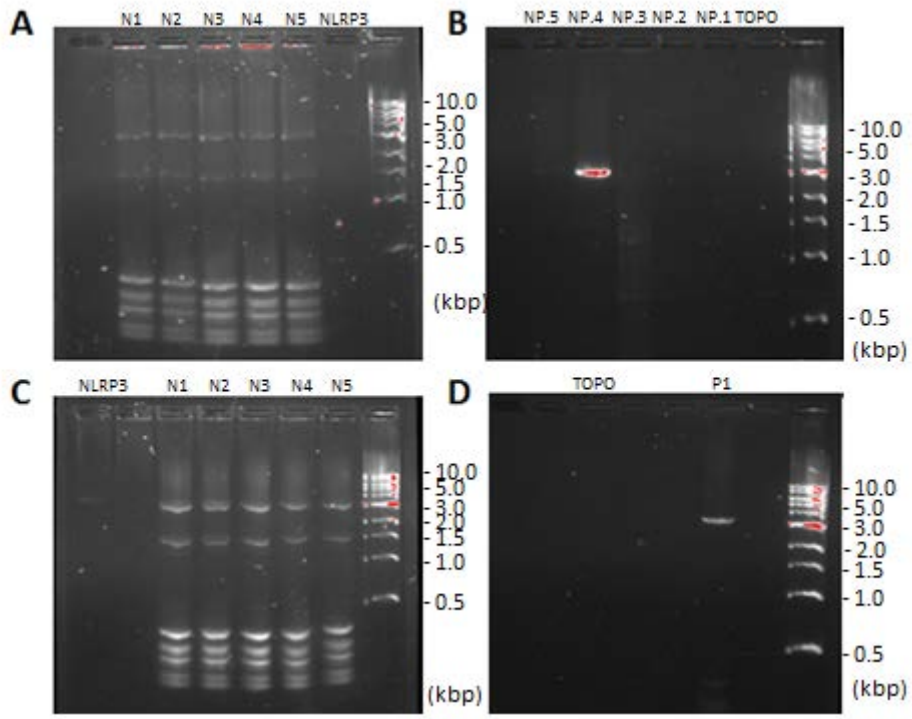

* N: NLRP3 PCR samples, NP/P: Plasmid with NLRP3 samples.

Figure 7. Result of agarose gel electrophoresis of PCR amplifications. 1kb Ladder (BiolabsA) Attempt to add overhangs to NLRP3, B) Successful NLRP3 amplification with overhangs performed with annealing temperature gradient (65°, 67.2°, 69°, **71.8°,** 72.9° C), C) Annealing temperature gradient (56°, 58.6°, 61.4°, 63.7°, 64.8° C) and attempt of NLRP3 amplification to add overhangs, D) Repeated PCR (71.8°C) to confirm result from picture B.

The designed TLR4 construct and the NLRP3 with added overhangs was set up to an OE-PCR with primers (NLRP3O_RP, TLR4_FP) and without primers for the strands to prime each other according to theory. All attempts with primers gave poor result with no amplification of the fusion product (Figure 8A, 8B). The PCR experiment which was performed without the presence of primers indicates successful fusion, with a fragment size around 3467 base pairs. The difference in size compared to the standard (NLRP3 with overhangs, Figure 8A, 8B – N3.O) was visible (Figure 8A, 8B – P3, P2, P1, FU, P1). Figure 8B also shows the attempts with fusion DNA and new DNA set up as template with primers which was still unsuccessful. All gels were run on a high voltage which resulted in poor separation of the 1 kb Ladder.

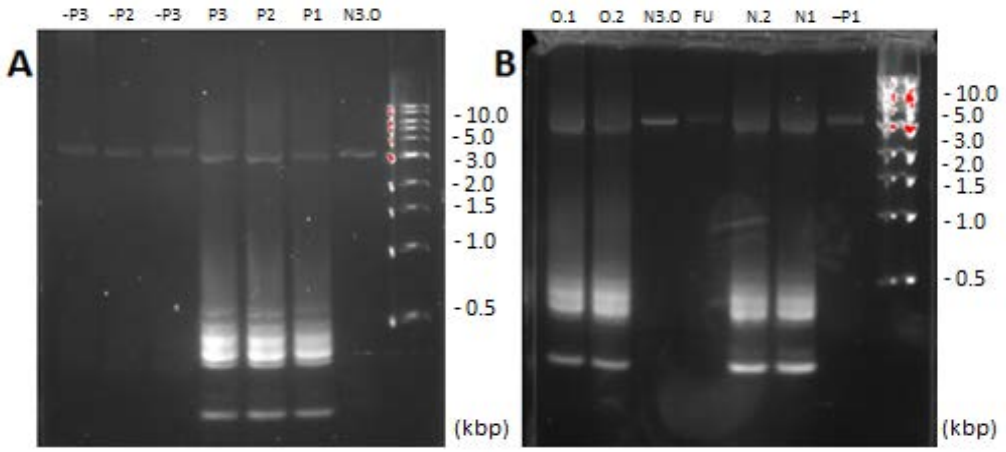

* -P: no primers, P: with primers, O: fusion product as template, FU: fusion product, N: new DNA set up

Figure 8. Result of agarose gel electrophoresis of PCR amplifications. 1kb Ladder (Biolabs) A) Attempt to create fusion protein with (P3, P2, P1) and without primers (-P3, -P2, -P3), B) Additional step to create fusion protein with new DNA samples without primers, new DNA (TLR4 & NLRP3) with primers and old PCR Fusion DNA. Figure 9

From the OE-PCR a potential fusion product was obtained and used for many amplification attempts. The fusion products from multiple PCR reactions were purified and pooled together. The pooled samples were used for digestion with Eam1104, ligation with pDUAL GC expression vector, transformed with DH5a- E.coli cells and then plated on kanamycin (100 µg/ml) plates. Control plates was made on both LB with and without kanamycin to ensure both the survival of the cells and that there was no resistance against the antibiotics. The control plates was successful but the cloning was unsuccessful and did not generate any colonies.

Table 9. Qubit and Nanodrop™ concentration and purity levels of only successful samples.

PCR Sample	**Qubit**		**NanoDrop™**		
	Concentration (ng/µl)	Attained amount (µg)	Concentration (ng/µl)	260/280	260/230
NLRP3	16.9	0.98	-	2.11	0.4
NLRP3 + overhangs	64.6	2.907	-	1.71	0.94
Fusion protein	6.54	0.189	-		

4. Discussion

To anchor the NLRP3 to the cell membrane was ambitious and not completed. The goal was to study the NLRP3 structure with the LPI technology. The NLRP3 was successfully amplified with the desired overhangs, and then fused with the designed TLR4 (Table 8B, 8D). The fusion product was obtained in limited amount and was insufficient for further processing.

A time-consuming part of PCR is to design the different oligonucleotides. The effort required is mandatory for success. When the TLR4 oligonucleotide was designed it included the transmembrane – part to anchor the NLRP3 to the membrane, the signal peptide which would relocate the NLRP3 to the right position, as well as different cutting sites for various proteases and enzymes. The design was 318 bp long and included a linker sequence for the overlap PCR. The enzymes, proteases and linker were chosen by recommendations in previous studies, but which was not essential in this specific fusion. It could be possible that the design needed more careful analysis to get a higher quality. Designing primers is one of the main factors which has the biggest impact on a PCR reaction. It will in most cases give better specificity and in turn a higher yield of amplified product (Chuang, Cheng, & Yang, 2013). Amplification requires primers that are specific to the binding site and it involves analysis of many different components and the search for right primers can be difficult (Ye et al., 2012). The amplification of the NLRP3 cDNA from the TOPO plasmid was efficient and the primers was designed accordingly to the coding region. As the NLRP3 was successfully amplified it was after purification used as template to add desired overhangs. However, when the overhangs were to be included and amplified, it was problematic which could have many different causing factors. The primers designed with NLRP3 overhangs had a length of 30-36 base pairs which can interfere with the amplification by self-binding or uncomplete elongation at wrong parameters (Roux, 2009). Already while mixing the PCR components the primers can bind in nonspecifically and the enzyme can in that case elongate these, creating undesired products (Spibida et al., 2017). The complications of the amplification resulted in the need to try different PCR programs. The complementarity of the primers was limited to only 8-12 base pairs the first cycles due to the added overhang which was still not included in the template. This lowered the annealing temperature of the primary cycles and then required a higher temperature after the whole primer had been included to the template.

While planning the fusion between the NLRP3 and parts of the TLR4, it was critical how the design was made, the efficiency of the reaction can often be effected by the compositions of the nucleotides, specifically GC-rich regions which can form self-dimers and create loop structures (Green & Sambrook, 2019). PCR is a well-established technique which over the years has been developed and optimized for PCR assays (Schrick & Nitsche, 2015). The primary PCR reactions were set without any large considerations e.g. the annealing temperature was not optimized for the primers used and time parameters not adjusted etc. The first PCR products gave gel result which did not show any distinct bands for either the NLRP3 or TLR4. PCR parameters was poorly optimized which can cause uncomplete digestion, lacking the presence of the desired fragments in the vector or unfit primers and failure to set the right PCR conditions can lead to undesired and undefined products (Roux, 2009). After certain adjustments to the PCR reaction, the concentration was higher within the range of 42.2 ng/µl – 85.2ng/µl. All samples were run on gel and the NLRP3 and TLR4 fragments produced a large smear and undesired fragments which can be caused by wrong annealing temperature, premature replication or incorrect template concentrations (PCR Troubleshooting Guide, New England BioLabs). The wrong annealing temperature is often one of the main factors to poor results and as new primers and new plasmids was used (TOPO, pQETRI),

the PCR was set with an annealing gradient. The gradient was used to find the temperature optimum for the specific primers. The NLRP3 bands were distinct on the gel (Figure 6) which indicates that the annealing temperature was more suitable for the NLRP3 primers than the TLR4 (Ye et al., 2012).

Amplification techniques that works efficiently in this case is both Touch-up PCR and Touch-down PCR. Compared to conventional PCR, these techniques adjust the annealing temperature to a higher or lower value than the target optimum. The touch-down starts at a higher temperature and is then gradually reduced to the optimum annealing temperature. The opposite which is Touch-up PCR is based on the principle that the initial cycling is set to a couple degrees below optimum and then increased (Rowther, Kardooni, & Warr, 2012). Touchdown PCR is used to decrease unspecific binding and the initial annealing temperature which is higher than optimum favors the amplification of desired fragment, creating target primer-template hybrids (Green & Sambrook, 2011). Different types of these two combined was used to investigate the optimum conditions for the overhang primers. As the annealing part to the template differ from the initial cycles and the remainder, the temperatures was set to different lower initial annealing temperature (55°C, 60°C) but which still was above the required optimum for the matching sequences (41-49°C), followed by a second annealing temperature (62° - 73° C) based on when the primers and template was matching (69° - 72.9° C). Different temperatures and gradients were used, and all results gave wrong fragment sizes indicating strong primer-dimer binding. The two different NLRP3_FP/2 primers were used in different program settings (Touch-up, touch-down, two-step) but no one came back with the desired results. Once more it highlights the importance of primer design and belonging properties as length, self-complementarity and GC% content. The amplification was then made with both the NLRP3 from previous amplification but also the TOPO plasmid as PCR template – which did give result. The PCR reaction of the plasmid together with the NLRP3_RP and NLRP3_FP2 gave a distinct band with the desired fragment size. As the reaction was run on different temperatures and only the 71.1° C was visible, the same procedure was repeated to confirm that it was a true result (Figure 7). Both attempts confirmed the desired size when run on gel (~3.2kb) which gave permission to move forward with the product.

By protein engineering the target protein and fusion protein are genetically linked together. Fusion proteins can be constructed to increase protein stability and expression, facilitate protein purification and detection or combine protein functions (Costa, Almeida, Castro, & Domingues, 2014). By performing and facilitate different mechanisms of a protein it additionally allows identification and various analyses of the target protein as quantification and e.g. structural studies. By creating a fusion protein, it can in some cases relocate the target protein to another cellular location. Genetically fused proteins rise wide opportunities in biological research for e.g. imaging and biopharmaceuticals. As the domains are fused the functionalities of both can be obtained and in many cases be an asset. When it comes to drug development – the targeting protein can by fusion cross biological barriers as cell membranes which in normal cases would not be possible (Malhotra, 2009; Butt, Edavettal, Hall, & Mattern, 2005). One approach when designing a fusion protein is to use linkers. Linkers is a peptide sequence which join the component proteins together. The linker often enhances the binding and help the proteins to correct folding, higher yield of protein production and unchanged protein function. The different composition and length can vary and result in different hydrophocity and propensity (i.e. ratio of amino acid occurrence in linker compared to full protein). Linkers have different functionalities; increasing stability, increasing expression, improving biological activity and more. Flexible linkers are often made of Glycine and Serine residues which are small and non-polar which optimal separation and maintains inter-domain interactions (Chen, Zaro, & Shen, 2012). Therefore, the

approach in designing the fusion gene was set with confident and the linker was clearly functioning as a fusion product was received.

OE-PCR was a time-efficient approach as well as cost-efficient. Ordering the full desired gene would cost a lot of money and that is why the project was based on already available plasmids. To execute the protein fusion, the two fragments was fused together by OE-PCR. There were two different approaches where it was possible to use one primer for each gene (e.g. TLR4_FP, NLRP3_RP) and to perform PCR without primers. All samples with primers showed unspecific binding by the high number of smaller fragments, while the samples without primers indicated the right fragment size (Figure 8). However, the concentrations were much lower as the lack of primers does not enable amplification. Multiple tries were made to receive a higher concentration but was not successful, which once more could be caused of poorly designed primers. The problem source of the primers could be due to the high self-complementarity and unfortunately brought effect to the outcome of the PCR reactions. After repeatedly efforts, the overlap PCR was run without primers and samples was pooled together so reach an efficient amount of fusion product. After purification, the pooled sample reached 6.54 ng/µl which was lower than desired. However, the sample was still used for further processing. There was an intense search of troubleshooting why the outcome was not as planned, and many things can be taken into consideration for further research (Table 13). The transformation with *E. coli*-DH5a-cells did not give any colonies. As the standard protocol for digestion and ligation require 1 µg of DNA it was an insufficient amount of DNA obtained prior these steps. Unfortunately, the outcome was highly effected, and the failure of the cloning demands further research to focus on obtaining a stable amount of fusion product. To receive a higher amount requires successful amplification with highly specific primers.

Table 13. Troubleshooting of PCR with relevant suggestions of cause.

Method	**Situation**	**Troubleshooting**	**Protocol reference**
PCR/Gel	Multiple bands	Too low annealing temperature, too short extension time, primer concentration too high	New England Biolabs ThermoFisher Scientific GenScript
	Low concentration	Too high annealing temperature, poor primer design, insufficient DNA quantity, problematic primer design	
	Smear	Excess DNA input, long targets, incorrect annealing temperature, insufficient extension	
	No product	Too high annealing temperature, wrong template, poor primer design	

5. Conclusion

The focus spent on oligonucleotide and PCR optimization was necessary but caused time-restrictions further down the project. The problematic situation due to the fact shows how crucial a proper design of both DNA and primers are for a successful implementation. The overlap PCR and all prior steps did give result and the fusion was performed. However, it was not possible to receive stable plasmid containing the desired fragment. While there is many different reasons why the cloning did not work there is of high belief that the insufficient amount of fusion product was responsible. Even though the fusion product was fused together there was lack of proof due to no conformational plasmid sequencing to prove so. Further research should use the fusion product as DNA template and try to sequence it prior usage and use the result for optimized primer design to ensure successful amplification of the product. Receiving a higher amount is crucial for secondary steps in the project and this will perhaps give purified plasmid containing the fusion gene which in turn can be used for insertion into mammalian cells and LPI™ technology.

6. Acknowledgements

First of all, I would like to thank Mikael Edjebäck for the chance to be a small part of their larger project. The insights have been a gain of knowledge greater than expected. Great thanks to my mentor Matthew Herring which has been contributing with generous help by discussions, guidance and advice through the whole project. Thank you for your great feedback and opinions and last, Magnus Fagerlind for your revision on my report which helped me to manage this bachelor thesis.

7. References

Ahn, J. H., Keum, J. W., & Kim, D. M. (2011). Expression screening of fusion partners from an E. coli genome for soluble expression of recombinant proteins in a cell-free protein synthesis system. *PloS one*, *6*(11), e26875. doi:10.1371/journal.pone.0026875

Baldwin, A.G., Tapia, V.S., Swanton, T., Beswick, J.A., Brough, D., & Freeman, S. (2018). Design, Synthesis and Evaluation of Oxazaborine Inhibitors of the NLRP3 Inflammasome. *ChemMedChem,* 13(4). https://doi.org/10.1002/cmdc.201700731

Butt, T.R., Edavettal, S.C., Hall, J.P.,& Mattern, M.R. (2005). SUMO fusion technology for difficult-to-express proteins. *Protein Expr Purif*, 43(1), pp. 1-9. doi:10.1016/j.pep.2005.03.016

Cassel, S. L. and Sutterwala, F. S. (2010), Sterile inflammatory responses mediated by the NLRP3 inflammasome. *Eur. J. Immunol*, 40 pp. 607-611. doi:10.1002/eji.200940207

Chen, X., Zaro, J. L., & Shen, W. C. (2012). Fusion protein linkers: property, design and functionality. *Advanced drug delivery reviews*, *65*(10), pp. 1357-69. doi: 10.1016/j.addr.2012.09.039

Chuang, L. Y., Cheng, Y.H., & Yang, C.H. (2013). Specific primer design for the polymerase chain reaction. *Biotechnol. Lett,* 35(10), pp.1541-1549. doi: 10.1007/s10529-013-1249-8

Costa, S., Almeida, A., Castro, A., & Domingues, L. (2014). Fusion tags for protein solubility, purification and immunogenicity in Escherichia coli: the novel Fh8 system. *Frontiers in microbiology*, *5*(63). doi:10.3389/fmicb.2014.00063

Davis, B.K., Wen, H., & Ting, J.P. (2011). The inflammasome NLRs in immunity, inflammation, and associated diseases. *Annual review of immunology*, *29*, pp. 707–735. doi:10.1146/annurev-immunol-031210-101405

Elliott, E.I., & Sutterwala, F.S. (2015). Initiation and perpetuation of NLRP3 inflammasome activation and assembly. *Immunological reviews*, *265*(1), pp. 35–52. doi:10.1111/imr.12286

Ellwanger, K., Becker, E., Kienes, I., Sowa, A., Postma, Y., Cardona Gloria, Y., & Kufer, T. A. (2018). The NLR family pyrin domain-containing 11 protein contributes to the regulation of inflammatory signaling. *The Journal of biological chemistry*, 293(8), pp. 2701–2710. doi:10.1074/jbc.RA117.000152

Estruch, M., Bancells, C., Beloki, L., Sanchez-Quesada, J.L., Ordonez-Llanos, J., & Benitez, S. (2013). CD14 and TLR4 mediate cytokine release promoted by electronegative LDL in monocytes. *Atherosclerosis,* 229(2), pp. 356-362. doi: 10.1016/j.atherosclerosis.2013.05.011.

Europaparlamentet. (2001). Europaparlamentets och rådets direktiv 2001/18/EG av den 12 mars 2001 om avsiktlig utsättning av genetiskt modifierade organismer i miljön och om upphävande av rådets direktiv 90/220/EEG - Kommissionens uttalande. *Europeiska gemenskapernas officiella tidning,* 106, pp. 1 – 39. Collected [24.01.2019] at https://eurlex.europa.eu/LexUriServ/LexUriServ.do?uri=CELEX:32001L0018:SV:HTML

Faustin B., Lartigue, L., Bruey J.M., Luciano, F., Sergienko, E., Bailly-Maitre, B., Volkamann, N., Hanein, D., Rouiller, L., & Reed, J.C. (2007). Reconstituted NALP1 inflammasome reveals two-step mechanism of caspase-1 activation. Mol Cell. 25, pp. 713–724. doi:10.1016/j.molcel.2007.01.032

Feldmann, J., Prieur, A.M., Quartier, P., Berquin, P., Certain, S., Cortis, E., Teillac-Hamel, D., Fischer, A., & de Saint Basile, G. (2002). Chronic infantile neurological cutaneous and articular syndrome is caused by mutations in CIAS1, a gene highly expressed in polymorphonuclear cells and chondrocytes. *Am J Hum Genet,* 71(1), pp. 198-203. doi:10.1086/341357

Franklin, B. S., Bossaller, L., De Nardo, D., Ratter, J. M., Stutz, A., Engels, G., … Latz, E. (2014). The adaptor ASC has extracellular and 'prionoid' activities that propagate inflammation. *Nature immunology*, *15*(8), pp. 727–737. doi:10.1038/ni.2913

Green, M.R., & Sambrook, J. (2018). Touchdown Polymerase Chain Reaction (PCR). *Cold Spring Harbor Protocols*. doi:10.1101/pdb.prot095133

Green, M.R., & Sambrook, J. (2019). Polymerase Chain Reaction (PCR) Amplification of GC-Rich Templates. *Cold Spring Harbor Protocols,* 2. doi: 10.1101/pdb.prot095141

Groslambert, M., & Py, B.F. (2018). Spotlight on the NLRP3 inflammasome pathway. *Journal of inflammation research*, 11, pp. 359-374. doi:10.2147/JIR.S141220

Hato, T., & Dagher, P.C. (2015) How the Innate Immune System Senses Trouble and Causes Trouble. *CJASN*, 10 (8), pp. 1459-1469. doi: 10.2215/CJN.04680514

Heckman, K.L., & Pease, L.R. (2007). Gene splicing and mutagenesis by PCR-driven overlap extension. *Nature Protocols*, 2, pp. 924-932. doi.org/10.1038/nprot.2007.132

Ho SN, Hunt HD, Horton RM, Pullen JK, Pease LR. (1989). Site-directed mutagenesis by overlap extension using the polymerase chain reaction. Gene. 1989;77(1):51–59. doi: 10.1016/0378-1119(89)90358-2

Hussain H, Chong NF. (2016). Combined Overlap Extension PCR Method for Improved Site Directed Mutagenesis. *Biomed Res Int.*:8041532. doi: 10.1155/2016/8041532.

Inoue, M., & Shinohara, M. L. (2013). NLRP3 Inflammasome and MS/EAE. *Autoimmune diseases*, *2013*, 859145. doi:10.1155/2013/859145

Jiang, H., He, H., Chen, Y., Huang, W., Cheng, J., Ye, J., & Zhou, R. (2017). Identification of a selective and direct NLRP3 inhibitor to treat inflammatory disorders. *The Journal of experimental medicine*, *214*(11), pp. 3219–3238. doi:10.1084/jem.20171419

Jo, E.K., Kim, J.K., Shin, D.M., & Sasakawa, C. (2015). Molecular mechanisms regulating NLRP3 inflammasome activation. *Cellular & molecular immunology*, *13*(2), pp. 148-159. doi:10.1038/cmi.2015.95

Liu, J., & Cao, X. (2016). Cellular and molecular regulation of innate inflammatory responses. *Cellular & molecular immunology*, *13*(6), pp. 711–721. doi:10.1038/cmi.2016.58

Luo, W. G., Liu, H. Z., Lin, W. H., Kabir, M. H., & Su, Y. (2013). Simultaneous splicing of multiple DNA fragments in one PCR reaction. *Biological procedures online*, *15*(1), 9. doi:10.1186/1480-9222-15-9

Malhotra A. (2009). "Tagging for protein expression". *Guide to Protein Purification* 2nd Edn eds Burgess R. R., Deutscher M. P., editors. (San Diego, CA: Elsevier;), 463, pp. 239–258 . doi: 10.1016/S0076-6879(09)63016-0

Manji, G.A., Wang, L., Geddes, B.J., Brown, M., Merriam, S., Al-Garawi, A., Mak, S., Lora, J.M., Briskin, M., Jurman, M., Cao, J., DiStefano, P.S., & Bertin, J. (2002). PYPAF1, a PYRIN-containing Apaf1-like protein that assembles with ASC and regulates activation of NF-kappa B. *J Biol Chem,* 277(13), pp. 11570-11575. doi:10.1074/jbc.M112208200

Medzhitov, R., Preston-Hurlburt, P., & Janeway, CA.Jr. (1997). A human homologue of the Drosophila Toll protein signals activation of adaptive immunity. *Nature,* 388(6640), pp. 394-397. doi:10.1038/41131

Miao, H., Ou, J., Ma, Y., Guo, F., Yang, Z., Wiggins, M., … Yu, L. (2014). Macrophage CGI-58 deficiency activates ROS-inflammasome pathway to promote insulin resistance in mice. *Cell reports*, *7*(1), pp. 223–235. doi:10.1016/j.celrep.2014.02.047

Moossavi, M., Parsamanesh, N., Bahrami, A., Atkin, S.L., & Sahebkar, A. (2018). Role of the NLRP3 inflammasome in cancer. *Molecular cancer*, *17*(1), pp. 158. doi:10.1186/s12943-018-0900-3

Nakanishi H, Kawashima Y, Kurima K, Chae JJ, Ross AM, Pinto-Patarroyo G, Patel SK, Muskett JA, Ratay, J.S., Chattaraj, P., Park, Y.H., Grevich, S., Brewer, C.C., Hoa, M., Kim, H.J., Butman, J.A., Broderick, L., Hoffman, H.M., Aksentijevich, I., Kastner, D.L., Goldbach-Mansky, R., & Griffith, A.J. (2017). NLRP3 mutation and cochlear autoinflammation cause syndromic and nonsyndromic hearing loss DFNA34 responsive to anakinra therapy. *Proc Natl Acad Sci U S A*, 12, pp. 114-137. doi: 10.1073/pnas.1702946114.

New England Biolabs. PCR Troubleshooting Guide. Collected [2019.03.29] at https://international.neb.com/tools-and-resources/troubleshooting-guides/pcr-troubleshooting-guide

Nicholson L. B. (2016). The immune system. *Essays in biochemistry*, *60*(3), pp. 275-301. https://doi.org/10.1042/EBC20160017

PCR Troubleshooting Guide. Genscript. Collected [2019.04.15] at https://www.genscript.com/pcr-troubleshooting-guide.html

Pearce, E.L., & Pearce, E.J. (2013). Metabolic pathways in immune cell activation and quiescence. *Immunity*, *38*(4), pp. 633–643. doi:10.1016/j.immuni.2013.04.005

Prame Kumar, K., Nicholls, A. J., & Wong, C. (2018). Partners in crime: neutrophils and monocytes/macrophages in inflammation and disease. *Cell and tissue research*, *371*(3), pp. 551–565. doi:10.1007/s00441-017-2753-2

Próchnicki, T., Mangan, M.S., & Latz, E. (2016). Recent insights into the molecular mechanisms of the NLRP3 inflammasome activation. *F1000Research*, *5*, F1000 Faculty Rev-1469. doi:10.12688/f1000research.8614.1

Roux, K.H. (2009). Optimization and troubleshooting in PCR. *Cold Spring Harb Protoc,* 4. doi: 10.1101/pdb.ip66

Rowther FB, Kardooni H, Warr T. (2012). TOUCH-UP gradient amplification method. *J Biomol Tech*, 20(1), pp. 1-3. doi: 10.7171/jbt.12-2301-004.

Schmidt, M., Raghavan, B., Mûller, V., Vogl, T., Fejer, G., Tchaptchet, S., Keck, S., Kalis, C., Nielsen, P.J., Galanos, C., Roth, J., Skerra, A., Martin, S.F., Freduenberg, M.A., & Goebeler, M. (2010). Crucial role for human Toll-like receptor 4 in the development of contact allergy to nickel. *Nat Immunol,* 11(9), pp. 814-819. doi: 10.1038/ni.1919.

Schrick, L., & Nitsche, A. (2015). Pitfalls in PCR troubleshooting: Expect the unexpected? *Biomolecular detection and quantification*, *6*, pp. 1–3. doi: 10.1016/j.bdq.2015.11.001

Shao, B. Z., Xu, Z. Q., Han, B. Z., Su, D. F., & Liu, C. (2015). NLRP3 inflammasome and its inhibitors: a review. *Frontiers in pharmacology*, *6*, pp. 262. doi:10.3389/fphar.2015.00262

Sheedy, F. J., Grebe, A., Rayner, K. J., Kalantari, P., Ramkhelawon, B., Carpenter, S. B., … Moore, K. J. (2013). CD36 coordinates NLRP3 inflammasome activation by facilitating intracellular nucleation

of soluble ligands into particulate ligands in sterile inflammation. *Nature immunology*, *14*(8), pp. 812–820. doi:10.1038/ni.2639

Shevchuk, N. A., Bryksin, A. V., Nusinovich, Y. A., Cabello, F. C., Sutherland, M., & Ladisch, S. (2004). Construction of long DNA molecules using long PCR-based fusion of several fragments simultaneously. *Nucleic acids research*, *32*(2), e19. doi:10.1093/nar/gnh014

Swedish Work Environment Authority. (2011). Contained Use of Genetically modified Microorganisms (AFS 2011:2Eng), provisions. Collected [05.02.2019] at https://www.av.se/en/workenvironmentworkandinspections/publications/foreskrifter/contained-use-of-genetically-modified-micro-organisms-afs-20112eng-provisions/

Tatematsu, M., Yoshida, R., Morioka, Y., Ishii, N., Funami, K., Watanabe, A., Saeki, K., & Seya, T., Matsumoto, M. (2016). Raftlin Controls Lipopolysaccharide-Induced TLR4 Internalization and TICAM-1 Signaling in a Cell Type-Specific Manner. *J Immunol.* 196(9), pp. 3865-3876. doi: 10.4049/jimmunol.1501734.

ThermoFisher Scientific. (2019). PCR Methods – Top Ten Strategies. Collected [2019.04.01] at https://www.thermofisher.com/se/en/home/life-science/cloning/cloning-learning-center/invitrogen-school-of-molecular-biology/pcr-education/pcr-reagents-enzymes/pcr-methods.html

Wacleche, V. S., Tremblay, C. L., Routy, J. P., & Ancuta, P. (2018). The Biology of Monocytes and Dendritic Cells: Contribution to HIV Pathogenesis. *Viruses*, *10*(2), pp. 65. doi:10.3390/v10020065

Yang, Y., Wang, H., Kouadir, M., Song, H., & Shi, F. (2019). Recent advances in the mechanisms of NLRP3 inflammasome activation and its inhibitors. *Cell death & disease*, *10*(2), pp. 128. doi:10.1038/s41419-019-1413-8v

Yatim, K.M., & Lakkis, F.G. (2015). A brief journey through the immune system. *Clinical journal of the American Society of Nephrology, 10*(7), pp. 1274-81. doi: 10.2215/CJN.10031014

Ye, J., Coulouris, G., Zaretskaya, I., Cutcutache, I., Rozen, S., & Madden, T. L. (2012). Primer-BLAST: a tool to design target-specific primers for polymerase chain reaction. *BMC bioinformatics*, *13*, pp. 134. doi:10.1186/1471-2105-13-134

Tools

Oligo Calc. Available at: http://biotools.nubic.northwestern.edu/OligoCalc.html

Primer Blast. Available at: https://www.ncbi.nlm.nih.gov/tools/primer-blast/

Reverse Complement. Available at: http://www.bioinformatics.org/sms/rev_comp.html

BLAST alignment. Available at: https://blast.ncbi.nlm.nih.gov/Blast.cgi?PROGRAM=blastn&PAGE_TYPE=BlastSearch&LINK_LOC=blasthome

ORF analyzer. Available at: http://www.geneius.de/GENEius/Orf_analyzeSequence.action

Primer3. Available at: http://biotools.umassmed.edu/bioapps/primer3_www.cgi

8. Appendices

8.1 Appendix 1 – NLRP3 sequence and feature keys

```
10         20         30         40         50
MKMASTRCKL ARYLEDLEDV DLKKFKMHLE DYPPQKGCIP LPRGQTEKAD
60         70         80         90         100
HVDLATLMID FNGEEKAWAM AVWIFAAINR RDLYEKAKRD EPKWGSDNAR
110        120        130        140        150
VSNPTVICQE DSIEEEWMGL LEYLSRISIC KMKKDYRKKY RKYVRSRFQC
160        170        180        190        200
IEDRNARLGE SVSLNKRYTR LRLIKEHRSQ QEREQELLAI GKTKTCESPV
210        220        230        240        250
SPIKMELLFD PDDEHSEPVH TVVFQGAAGI GKTILARKMM LDWASGTLYQ
260        270        280        290        300
DRFDYLFYIH CREVSLVTQR SLGDLIMSCC PDPNPPIHKI VRKPSRILFL
310        320        330        340        350
MDGFDELQGA FDEHIGPLCT DWQKAERGDI LLSSLIRKKL LPEASLLITT
360        370        380        390        400
RPVALEKLQH LLDHPRHVEI LGFSEAKRKE YFFKYFSDEA QARAAFSLIQ
410        420        430        440        450
ENEVLFTMCF IPLVCWIVCT GLKQQMESGK SLAQTSKTTT AVYVFFLSSL
460        470        480        490        500
LQPRGGSQEH GLCAHLWGLC SLAADGIWNQ KILFEESDLR NHGLQKADVS
510        520        530        540        550
AFLRMNLFQK EVDCEKFYSF IHMTFQEFFA AMYYLLEEEK EGRTNVPGSR
560        570        580        590        600
LKLPSRDVTV LLENYGKFEK GYLIFVVRFL FGLVNQERTS YLEKKLSCKI
610        620        630        640        650
SQQIRLELLK WIEVKAKAKK LQIQPSQLEL FYCLYEMQEE DFVQRAMDYF
660        670        680        690        700
PKIEINLSTR MDHMVSSFCI ENCHRVESLS LGFLHNMPKE EEEEEKEGRH
710        720        730        740        750
LDMVQCVLPS SSHAACSHGL VNSHLTSSFC RGLFSVLSTS QSLTELDLSD
760        770        780        790        800
NSLGDPGMRV LCETLQHPGC NIRRLWLGRC GLSHECCFDI SLVLSSNQKL
810        820        830        840        850
VELDLSDNAL GDFGIRLLCV GLKHLLCNLK KLWLVSCCLT SACCQDLASV
860        870        880        890        900
LSTSHSLTRL YVGENALGDS GVAILCEKAK NPQCNLQKLG LVNSGLTSVC
910        920        930        940        950
CSALSSVLST NQNLTHLYLR GNTLGDKGIK LLCEGLLHPD CKLQVLELDN
960        970        980        990        1000
CNLTSHCCWD LSTLLTSSQS LRKLSLGNND LGDLGVMMFC EVLKQQSCLL
1010       1020       1030
QNLGLSEMYF NYETKSALET LQEEKPELTV VFEPSW
```

NLRP3 human sequence. Chain intracellular. Blue= Pyrin. Yellow= NACHT. Green= Compositional bias. Grey= LRR 1-9. Collected [2019.01.25]https://www.uniprot.org/blast/?about=Q96P20[11036]&key=Chain&id=PRO_0000080886

8.2 TL4 amino acid sequence

```
10          20          30          40          50
MMSASRLAGT LIPAMAFLSC VRPESWEPCV EVVPNITYQC MELNFYKIPD
60          70          80          90          100
NLPFSTKNLD LSFNPLRHLG SYSFFSFPEL QVLDLSRCEI QTIEDGAYQS
110         120         130         140         150
LSHLSTLILT GNPIQSLALG AFSGLSSLQK LVAVETNLAS LENFPIGHLK
160         170         180         190         200
TLKELNVAHN LIQSFKLPEY FSNLTNLEHL DLSSNKIQSI YCTDLRVLHQ
210         220         230         240         250
MPLLNLSLDL SLNPMNFIQP GAFKEIRLHK LTLRNNFDSL NVMKTCIQGL
260         270         280         290         300
AGLEVHRLVL GEFRNEGNLE KFDKSALEGL CNLTIEEFRL AYLDYYLDDI
310         320         330         340         350
IDLFNCLTNV SSFSLVSVTI ERVKDFSYNF GWQHLELVNC KFGQFPTLKL
360         370         380         390         400
KSLKRLTFTS NKGGNAFSEV DLPSLEFLDL SRNGLSFKGC CSQSDFGTTS
410         420         430         440         450
LKYLDLSFNG VITMSSNFLG LEQLEHLDFQ HSNLKQMSEF SVFLSLRNLI
460         470         480         490         500
YLDISHTHTR VAFNGIFNGL SSLEVLKMAG NSFQENFLPD IFTELRNLTF
510         520         530         540         550
LDLSQCQLEQ LSPTAFNSLS SLQVLNMSHN NFFSLDTFPY KCLNSLQVLD
560         570         580         590         600
YSLNHIMTSK KQELQHFPSS LAFLNLTQND FACTCEHQSF LQWIKDQRQL
610         620         630         640         650
LVEVERMECA TPSDKQGMPV LSLNITCQMN KTIIGVSVLS VLVVSVVAVL
660         670         680         690         700
VYKFYFHLML LAGC IKYGRG ENIYDAFVIY SSQDEDWVRN ELVKNLEEGV
710         720         730         740         750
PPFQLCLHYR DFIPGVAIAA NIIHEGFHKS RKVIVVVSQH FIQSRWCIFE
760         770         780         790         800
YEIAQTWQFL SSRAGIIFIV LQKVEKTLLR QQVELYRLLS RNTYLEWEDS
810         820         830
VLGRHIFWRR LRKALLDGKS WNPEGTVGTG CNWQEATSI
```

Grey= Signal peptide. Blue= Extracellular. Green= Transmembrane. Orange= Intracellular. Collected [2019.01.26]
https://www.uniprot.org/blast/?about=O00206[632-652]&key=Transmembrane

8.3 Appendix 2: Buffer and solution composition

100ml TAE Buffer 50X stock
24.2g Tris base
Acetate (acetic acid) 5.71 ml(17.4M)
10ml EDTA 0.5M
Add dH_2O to 100ml
1X = 20ml stock solution + 980ml dH_20

LB Medium with/without antibiotic & agar 1l
10g/L tryptone
5g/L yeast extract
10g/L NaCl
+ Autoclaving, 100µg/ml ampicillin
15g agar/l

1% Agarose gel
100ml TAE Buffer
1g Agarose
Microwave 1-3min

10 000X GelRed add to 1X,

30 ml EDTA 0.5 M EDTA (pH 8.0)
5.6g disodium EDTA
25ml dH_20
Adjust pH with magnetic stirrer– fill with water
Autoclave

Separating 15% polyacrylamide gel
3.65 ml deionized water
3.75 ml 40% acrylamide/bis-acrylamide
2.5 ml 1.5 M Tris-HCl pH 8.8
0.1 ml 10 % SDS
50 µl 10% APS
5 µl TEMED

Stacking 4% polyacrylamide gel
3.2 ml deionized water
0.5 ml 40% acrylamide/bis-acrylamide
1.25 ml 0.5 M Tris-HCl pH 6.8
0.05 ml 10% SDS
25 µl 10% APS
5 µl TEMED

TBS 10X 75ml
1.8 g Tris base
6.6 g NaCl
Adjust pH to 7.6 with HCl
Add dH_20 up to 75 ml

TBST
50 ml 10X TBS
0.5ml Tween
Add dH_2O to 500 ml
For 5 % skim milk + TBST: 50 ml TBST & 2.5g milk powder

PBST
0.8 g NaCl
0.02 g KCl
0.144 g Disodium phosphate
0.024 g Monopotassium phosphate
0.2 ml Tween
Adjust pH to 7.2 with HCl
Add dH_20 to 100 ml

Kits

QIAquick Gel Extractions
PureYield plasmid purification
QIAprep Spin Miniprep Kit
Wizard SV Gel and PCR Clean-up System
Digestion Eam 1104
Ligation T4 DNA Ligase protocol
Library Efficiency DH5a Competent Cells
Subcloning Efficiency DH5a Competent Cells
Qubit dsDNA BR Assay Kits

8.4 Unsuccessful PCR gel pictures